Forest fire monitoring using NOAA satellite AVHRR

M. D. FLANNIGAN
Canadian Forestry Service, Petawawa National Forestry Institute, Chalk River, Ont., Canada K0J 1J0
AND
T. H. VONDER HAAR
Department of Atmospheric Science, Colorado State University, Fort Collins, CO, U.S.A. 80523

Received December 2, 1985[1]
Accepted May 16, 1986

FLANNIGAN, M. D., and T. H. VONDER HAAR. 1986. Forest fire monitoring using NOAA satellite AVHRR. Can. J. For. Res. **16**: 975–982.

The feasibility of using the advanced very high resolution radiometer (AVHRR) carried by the National Oceanic and Atmospheric Administration (NOAA) series of satellites to monitor forest fires was tested during a severe fire outbreak in north central Alberta between June 12 and June 21, 1982. A multispectral technique used AVHRR channels 3 and 4 to identify fires and estimate fire size. This multispectral approach enabled identification of subpixel-sized fires as small as 1 ha. During the study, fires were obscured from satellite view by the presence of cloud and smoke 59% of the time. In the remaining time, 80% of the fires listed by the Alberta Forest Service were identified by satellite. Satellite observations of forest fires are not sufficiently accurate to replace existing monitoring methods, but they are of value in providing a rapid, inexpensive supplement, especially in remote forested areas.

FLANNIGAN, M. D., et T. H. VONDER HAAR. 1986. Forest fire monitoring using NOAA satellite AVHRR. Can. J. For. Res. **16**: 975–982.

La faisabilité de surveiller les incendies de forêt à l'aide du radiomètre perfectionné à très haut pouvoir de résolution (AVHRR), embarqué par les séries de satellites de la National Oceanic and Atmospheric Administration (NOAA), a été testée lors d'un début d'incendie sévère dans le centre-nord de l'Alberta entre le 12 et le 21 juin 1982. Une technique multispectrale utilisant les canaux 3 et 4 du radiomètre a été employée pour reconnaître les incendies et estimer leur superficie. Cette technique a permis de repérer des incendies de superficie aussi faible que 1 ha, couvrant moins d'un pixel. Au cours de l'étude, la présence de nuages et de fumées a voilé les incendies pour le radiomètre 59% du temps. Le reste du temps, 80% des incendies relevés par le service des forêts de l'Alberta ont été repérés par le radiomètre. L'observation des feux de forêt par les satellites n'est pas assez précise pour remplacer les méthodes actuelles de surveillance, mais elle constitue un complément rapide et peu coûteux, surtout pour les régions forestières éloignées.

[Traduit par la revue]

Introduction

Forest fires are a major concern in Canada where, in a single year, up to 5.3 million ha may burn and control costs may exceed $135 million (Ramsey and Higgins 1985). Early detection of forest fires is imperative if control is to succeed. Manned towers and aircraft reconnaissance could be used for fire detection over vast areas of Canada's forest but would be inordinately expensive if conducted at the density and frequency for optimum fire control. This is particularly true over areas of low fire control priority where observations by conventional means are usually infrequent. Observations from a National Oceanic and Atmospheric Administration (NOAA) satellite series using the advanced very high resolution radiometer (AVHRR) can be used to examine extensive land areas two to four times each day depending on the number of NOAA satellites in operation. In this paper, the potential contribution of the NOAA satellite series to fire identification and size estimation is discussed.

Satellite monitoring of forest fires has been possible for over two decades. Every day the earth is observed by a growing number of satellites, but only a small percentage of these observations are appropriate for monitoring forest fires. For example, Landsat 5, with a resolution of 30 m, would be ideal for fire monitoring were it not for the 16-day gap between passes over the same area. However, Landsat data have been used to calculate area burned by a fire in Alaska after the fire was extinguished (Hall et al. 1979). The Geostationary Operational Environmental Satellite (GOES), which is excellent in terms of frequency of observations (every 30 min), has three major drawbacks: first, the resolution in the infrared channel is only 7 km at nadir, making it impossible to detect small fires; second, GOES has only one infrared channel, thereby eliminating the possibility of a multispectral approach[2]; and third, GOES is of limited value north of 60° N because of a loss of resolution caused by the curvature of the earth (Clark 1983). However, it has been possible to detect fires indirectly by using the higher resolution (0.9 km at nadir) GOES visible channel to spot smoke plumes from larger fires. The best observational system for forest fire monitoring is that carried out by the NOAA satellites. It allows multispectral sampling (two or three infrared channels), enabling identification of small fires, and monitors the same area two to four times a day.

Data

AVHRR

The NOAA satellites were designed to operate in a near-polar, sun-synchronous orbit at a nominal altitude of 833 km such that the local solar time of the satellite's passage remains essentially unchanged for any latitude. The orbital period is 104 min, which results in 14.2 orbits per day. The NOAA satellite series has a payload of six instruments, including the AVHRR. The AVHRR, on board NOAA satellites since 1979,

[1]Revised manuscript received May 12, 1986.

[2]Future GOES-I,J,K satellites will have multispectral capabilities as does the present VAS (VISSR (visible and infrared spin–scan radiometer) atmospheric sounder) experiment on GOES.

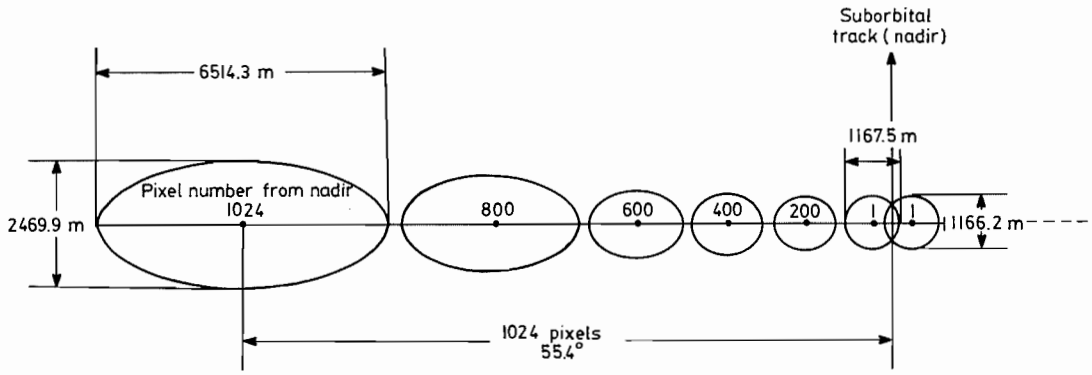

FIG. 1. Relative sizes of selected pixels along a AVHRR scan line as projected on the Earth (from Tappan and Miller 1982).

TABLE 1. Bandwidth and IFOV of the AVHRR

Channel	Bandwidth (μm) NOAA-6, NOAA-8	Bandwidth (μm) NOAA-7, NOAA-9	IFOV (mrad)
1	0.58–0.68	0.58–0.68	1.39
2	0.725–1.10	0.725–1.10	1.41
3	3.55–3.93	3.55–3.93	1.51
4	10.5–11.5	10.5–11.3	1.41
5	10.5–11.5	11.5–12.5	1.3

is a cross-track spin–scan radiometer with a scan rate of 360 rotations per minute. It records data within an angle of ±55.4° from nadir, equivalent to a swath width of 2600 km. Data are digitized on board the spacecraft at a rate of 2048 samples per scan per channel. The AVHRR provides one visible channel, one near-infrared channel, and two or three infrared channels (Kidwell 1984) (Table 1).

The instantaneous field of view (IFOV) for all AVHRR channels is given in Table 1. The IFOV of each channel is approximately 1.4 mrad, representing a picture element (pixel) diameter of about 1.16 km at nadir for a nominal altitude of 833 km. The constant IFOV causes pixels along a scan line to become larger with respect to ground as distance increases from nadir. Also, the pixel's shape changes from nearly circular at nadir to highly elliptical at the extremities of the view angle (Fig. 1).

The wavelengths for each channel were designed to coincide with regions of atmospheric transparency (atmospheric windows). Two or more channels provide independent sets of observations for the determination of hydrologic, oceanographic, and meteorologic variables. For example, the data from multiple channels can provide an accurate measurement of sea surface temperature and discriminate between snow, ground, ice, or surface water. A complete description of the NOAA satellite series and the AVHRR can be found in Schwalb (1978, 1982) and Kidwell (1984).

NOAA-7 AVHRR data were obtained from the Atmospheric Environment Service ground station in Edmonton, Alta. The pass number, date, and start time (Mountain Daylight Time (MDT)) of each pass are shown in Table 2. Data were retrieved from two passes a day with the exception of days on which data were not available. Only data for viewing angles less than 40° from nadir were used. The ascending orbit (north-bound equator crossing) for NOAA-7 occurred in the region of interest during the afternoon, whereas the descending orbit occurred in the early morning. Usually there are two NOAA satellites in orbit,

TABLE 2. NOAA-7 AVHRR data

Pass No.	Date, 1982	Time (MDT)
5003	June 12	1453
5011	June 13	0449
5017	June 13	1441
5025	June 14	0437
5039	June 15	0425
5046	June 15	1558
5054	June 16	0554
5074	June 17	1534
5082	June 18	0530
5088	June 18	1522
5096	June 19	0518
5102	June 19	1510
5110	June 20	0506
5116	June 20	1459
5124	June 21	0454
5130	June 21	1447

which provide four passes a day, occurring approximately every 6 h.

The AVHRR data recorded by the Edmonton ground station included only three channels of the five transmitted. Of these, channel 2 was in the near infrared and channels 3 and 4 were in the infrared (Table 1). The detectors for each channel undergo a prelaunch calibration and the infrared detectors receive an additional calibration in orbit (Lauritson et al. 1979).

Fire occurrence

The satellite and forestry data for the period June 12 to June 21, 1982, were chosen to take advantage of a rapidly changing forest fire situation in the Slave Lake Forest Region in north central Alberta (Fig. 2). On June 12 only a few small fires were burning in the Slave Lake Forest Region. By June 21 there were over 30 fires burning out of control, some exceeding 20 000 ha in size.

The Slave Lake Forest Region, part of the boreal forest, extends from 54.5° N to 57.5° N and from 113° W to 117° W; it contains the following species: aspen (*Populus tremuloides* Michx.), balsam poplar (*Populus balsamifera* L.), lodgepole pine (*Pinus contorta* Dougl.), white spruce (*Picea glauca* (Moench.) Voss), and black spruce (*Picea mariana* (Mill.) B.S.P.). The mixture of species at any one location is dependent upon site conditions and recent stand history.

The forest fire data for this region were supplied by the Alberta Forest Service. The data, in the form of daily reports,

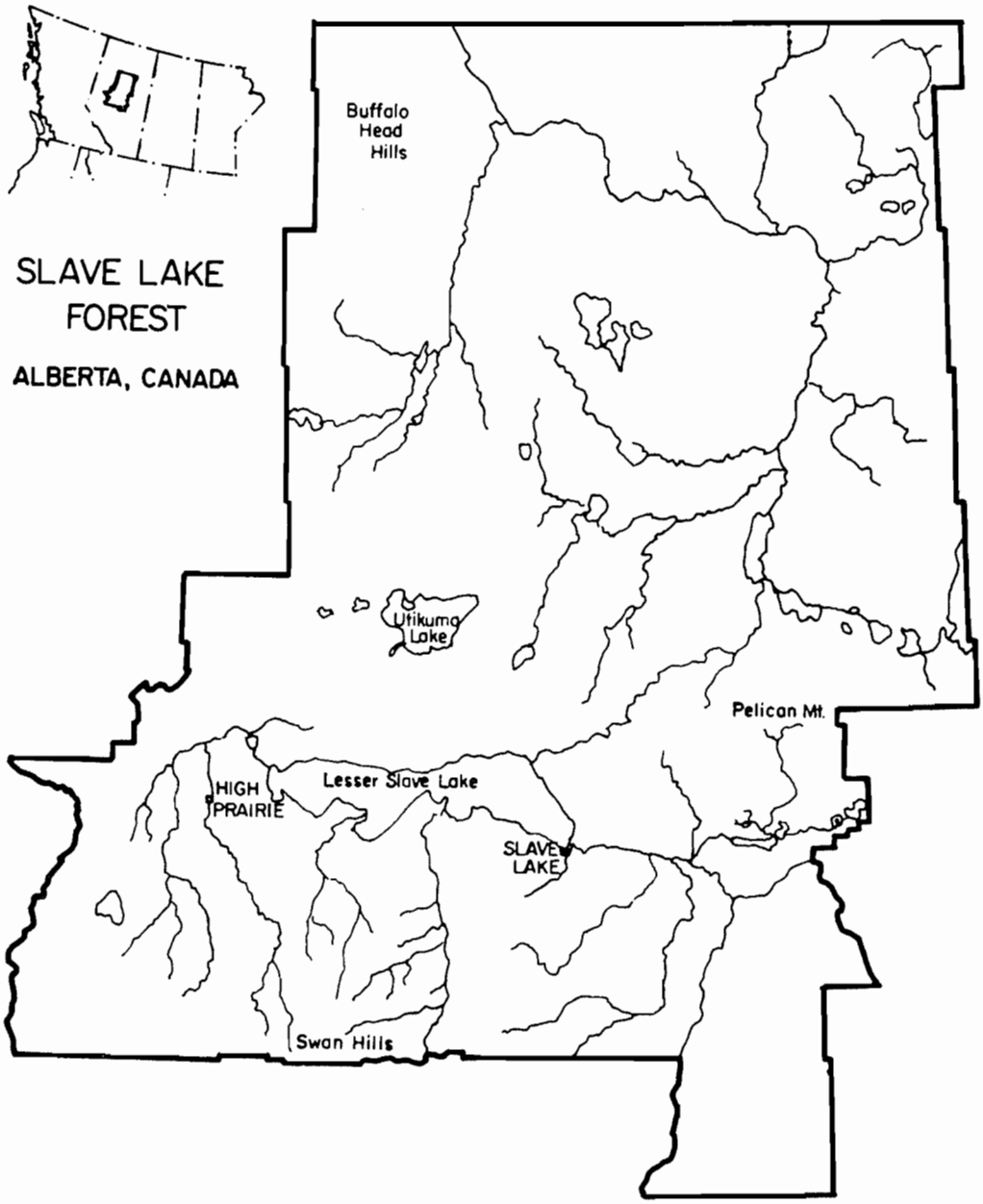

FIG. 2. The Slave Lake Forest Region in north central Alberta.

list by forest region, the name, location, size, and status of the fire, and resources in terms of men and equipment committed to control the fire. Almost all fires studied were ignited by lightning and only a few by humans. The location and size of each fire was determined usually by a late afternoon or early evening (1600–2000 MDT) aerial reconnaissance.

Satellite observations of fire

Dozier (1981) developed a technique using AVHRR channels 3 and 4 to find the temperature of a heat source and the percentage of the pixel covered by a hot target. Matson and Dozier (1981) used this multispectral approach to identify steel mills in the midwestern United States and gas flares from oil fields in the Middle East. The U.S. National Weather Service has used the infrared channels from the NOAA satellites since 1981 to help identify forest fires in the western United States (Matson et al. 1984).

Procedure

The analysis and calibration of satellite data was done at Colorado State University (CSU) on a DEC VAX 11-780 computer. Image display and processing was also done at the Department of Atmospheric Science at CSU on a COMTAL VISION ONE/20 terminal.

To calculate fire size and temperature within a pixel as viewed by the satellite, we used Dozier's (1981) multispectral approach. We can let $N_3(T_3)$ and $N_4(T_4)$ represent NOAA-7 channels 3 and 4 radiances sensed by the satellite. Radiance has the units of energy per area per time per frequency per steradian. The radiance is calculated by Planck's function and is dependent on the wavelengths of each channel and on the temperature of the viewed area. A pixel may be composed of a heat source, in this case a forest fire at temperature T_f that occupies portion p of the pixel (where $0 \leq p \leq 1$). The remaining portion $(1 - p)$ of the pixel is covered by forest with an assumed blackbody temperature T_b. By assuming that radiances sensed by channels 3 and 4 were independent of both the local solar zenith angle and the azimuth angle between the sun and satellite, we can write

$$[1] \quad N_3(T_3) = pN_3(T_f) + (1 - p)N_3(T_b)$$

$$[2] \quad N_4(T_4) = pN_4(T_f) + (1 - p)N_4(T_b)$$

where $N_3(T_3)$ and $N_4(T_4)$ are known. Once T_b is found by sampling nearby pixels, then $N_3(T_b)$ and $N_4(T_b)$ are calculated before p and T_f can be found by simultaneous solution of the two equations. By rearranging and substitution, the two equations are reduced to a single equation and then solved by iteration using inverse interpolation (Hornbeck 1975).

The contamination of daytime channel 3 data by reflected solar radiation constitutes a potential source of error that led, traditionally, to elimination of the use of the channel during daylight hours (Deschamps and Phulpin 1980; Llewelyn-Jones et al. 1984). Although less than 1% of solar radiation is received in the 3.5–4.0μm region, this amount intercepted by a surface is of the same order of magnitude as the radiation emitted by the surface (Hillger 1983; Llewelyn-Jones et al. 1984). Pixels that contain some cloud are assumed to be contaminated by the reflection of solar radiation at 3.5–4.0 μm based on the albedo of clouds (Kondrat'ev 1973; Bell and Wong 1981). Such pixels were identified by the cloud discrimination technique of Coakley and Bretherton (1982) and discarded.

In cloud-free areas, the albedo of the forest in the 3.5–4.0 μm region was required to determine if the data were contaminated. Although little information is available on the albedo of the forest in this wavelength region, Lee (1978) was able to show the reflectivity, absorption, and transmissivity of a typical hardwood leaf (Fig. 3) based on data from Gates (1965). Figure 3 shows that in the wavelength range 3.5–4.0 μm, there is total absorption and no reflection. Further evidence is provided by Wong and Blevin (1967), who studied reflectances of plant leaves and found that for wavelengths greater than 3.0 μm, reflectances are less than 0.05 for the majority of leaves. It is concluded that the amount of solar radiation reflected by the forest in the channel 3 wavelength region is insignificant and, therefore, channel 3 data can be used during daylight hours.

The differences in the radiometric response of AVHRR channels 3 and 4 wavelengths allow high temperature areas such as forest fires to be identified. Curves of Planck's function versus wavelength for a number of emitting temperatures are shown in Fig. 4. It is evident that the blackbody radiance increases with temperature and that the wavelength of maximum radiances decreases with increasing temperature. For a given increase in temperature, the fractional increase in area under the channel 3 section of the curves is greater than that under the channel 4 section. Therefore, the effective infrared temperature of a pixel with a fire present will be significantly higher for channel 3 as compared with channel 4. Fire pixels can be identified this way.

The identification of fire was accomplished for each pixel through a temperature differentiation technique. The effective infrared temperature of each cloud-free pixel was calculated for both channels 3 and 4. If the calculated temperature exceeded the mean background temperature of the forest and if the channel 3 temperature was greater than that of channel 4 by a critical value, fire was assumed to be present. Selected threshold values for the temperature differences were 8 K for night passes and 10 K for day passes. Plots of channel 3 and 4 temperatures along line 131 of NOAA-7 pass 5102 are shown in Fig. 5 and the corresponding images are shown in Figs. 6 and 7, respectively. The presence of a forest fire near pixel 325 is clearly indicated by the large difference in the response of the two channels. Contiguous pixels indicating fire presence were grouped together as one fire. The fire area in any given pixel was calculated by the described multispectral technique, except for areas in which a fire pixel was surrounded by other fire pixels. In such a case, it was assumed that the pixel represented an area which was totally burned (Flannigan 1985).

Three class sizes were chosen for verification of the fire identification technique; class 1, <4 ha; class 2, 4–40 ha; class 3, >40 ha; however, because of small sample sizes in classes 1 and 2, verification of fire size estimates were in only two categories, less than or greater than 400 ha. Actual fire sizes ranged from 0.5 to over 20 000 ha. Day and night passes were analyzed separately.

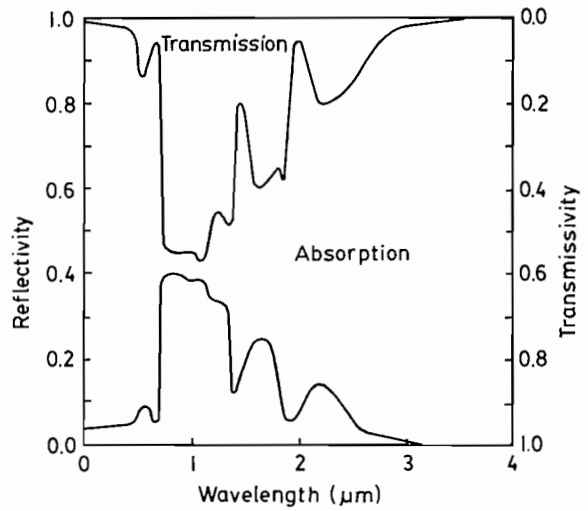

FIG. 3. Transmissivity, reflectivity, and absorptivity of a typical hardwood leaf (from Lee, 1978, based on data from Gates, 1965).

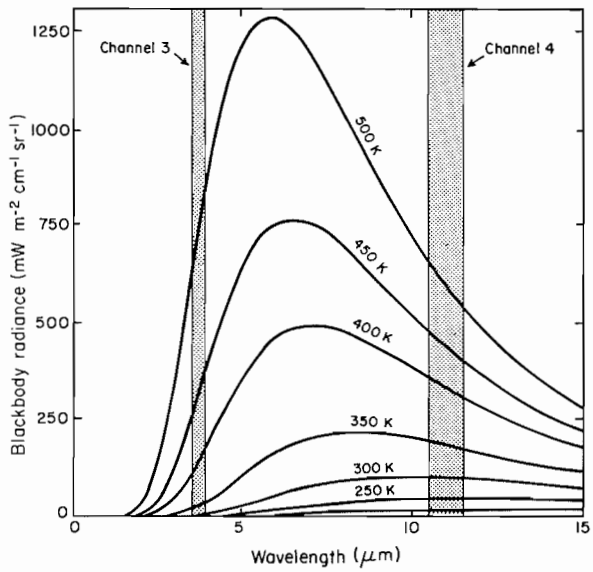

FIG. 4. Planck radiances for temperatures from 200 to 500 K (from Matson et al. 1984).

Results

Examples of processed channel 3 and 4 imagery for the same 360 thousand km^2 (600 km × 600 km) region are shown in Figs. 6 and 7. The enhancement scale is such that black represents warm temperatures and white represents cool temperatures. An example of solar contamination is evident in Fig. 6 where the clouds located near the center of the image appear warm (black) because of reflected solar radiation. The same clouds appear cool (white) on Fig. 7, as one would expect, because there is no significant solar radiation at the longer wavelengths. North of the cloud field one of many forest fires has been identified in Fig. 6. Not all black areas in Fig. 6 are forest fires. Some are agricultural areas such as the Peace River district on the left side of the image and some are burns from previous years such as the large black area on the upper right of the image.

In this investigation we have defined a "fire observation" as an occasion when fire, as reported by the Alberta Forestry Service, was present during a satellite pass. During this study

TABLE 3. Fraction* of total fire observations visible to the satellite

	Class 1 (<4 ha)	Class 2 (4–40 ha)	Class 3 (>40 ha)	Total
Day	7/36 (19%)	9/30 (30%)	62/117 (53%)	78/183 (43%)
Night	5/32 (16%)	15/41 (37%)	49/99 (49%)	69/172 (40%)
Total	12/68 (18%)	24/71 (34%)	111/216 (51%)	147/355 (41%)

*Number of fire observations visible to the satellite/total fire observations.

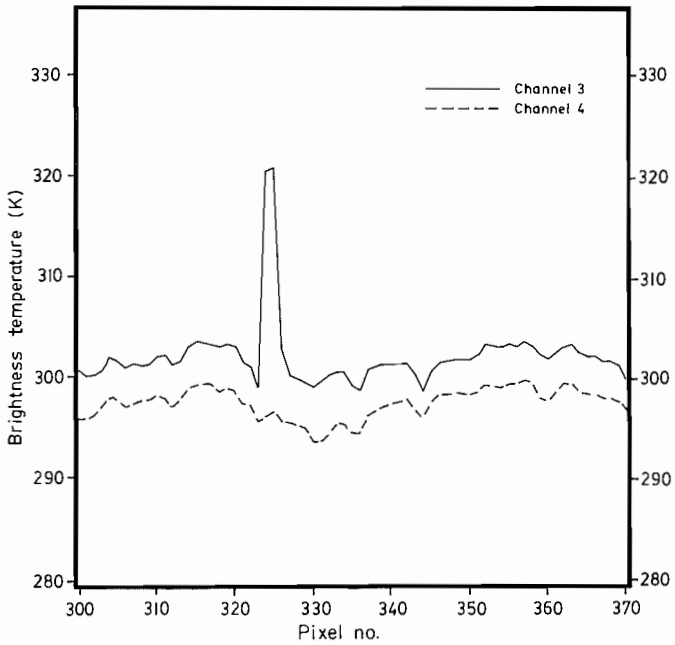

FIG. 5. Channel 3 and 4 brightness temperature plot along scan line 131 of NOAA-7 pass 5102 (the images for pass 5102 on channels 3 and 4 are shown in Figs. 6 and 7, respectively).

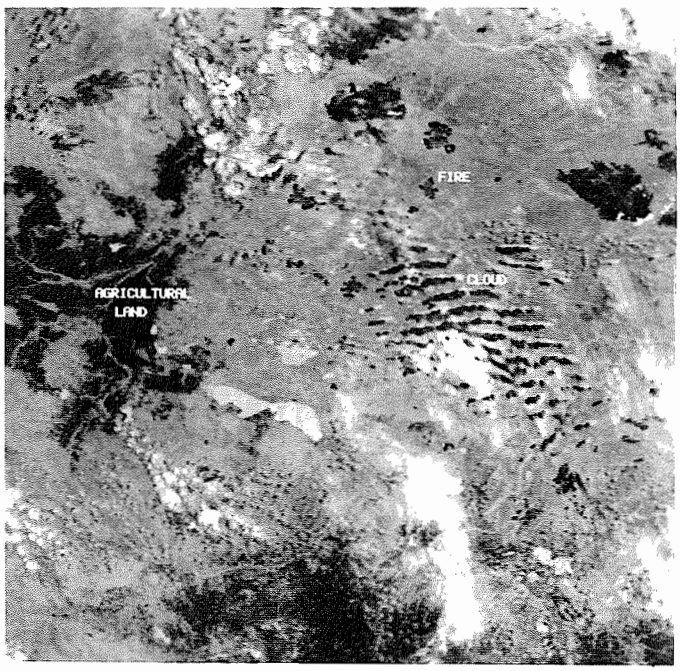

FIG. 6. NOAA-7 pass 5102, AVHRR channel 3, June 19, 1982, 1510 MDT, covering the Slave Lake Forest Region.

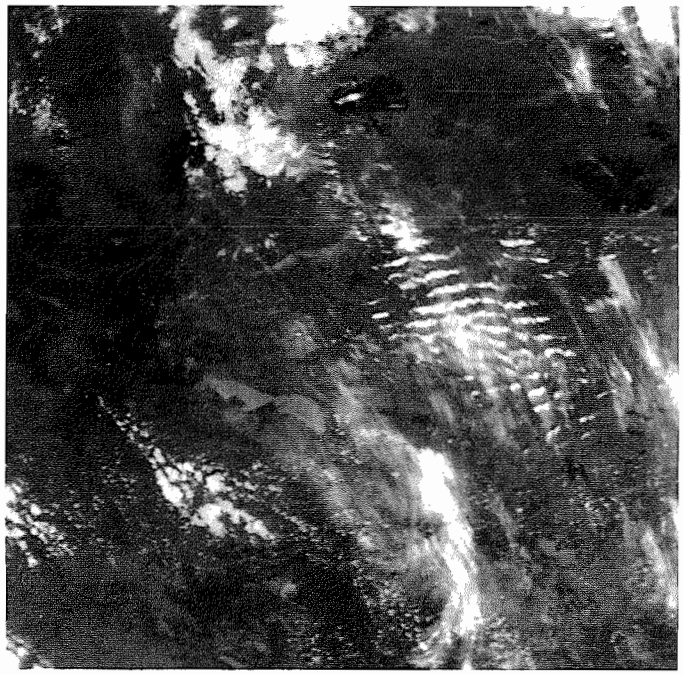

FIG. 7. NOAA-7 pass 5102, AVHRR channel 4, June 19, 1982, 1510 MDT, covering the Slave Lake Forest Region.

there was a total of 355 fire observations. This was taken as "ground truth." Of this total, many were repeat observations of the same fire. Table 3 shows that only 41% (147 of 355) of the total fire observations were visible to the satellite. The remainder were obscured by smoke and cloud. The fraction of potential day and night observations was about the same. Fifty-one percent of the largest fires were observable versus only 34% for class 2 and 18% for class 1.

Only 33% (118 of 355) of the total fire observations were actually identified by satellite (Table 4). For the smaller fires the percentage was 12–14%, increasing to 46% for the larger fires. A greater percentage of fire observations was identified during the day (37%) as compared with the night observations (29%). The better performance of fire identification during the day (afternoon passes) can be accounted for by the generally more vigorous burning as a result of lower relative humidities, higher temperatures, and stronger winds during the day.

The fraction of unobstructed fire observations identified by satellite is shown in Table 5. Of the fire observations without cloud and smoke cover, 80% were identified. Once again, the larger fires had a higher percentage identified (90%) as compared with the smaller fires (42–75%). A greater percentage of unobstructed fire observations were identified during the day (87%) than during the night (73%).

TABLE 4. Fraction* of total fire observations identified by satellite.

	Class 1 (<4 ha)	Class 2 (4–40 ha)	Class 3 (>40 ha)	Total
Day	4/36 (11%)	5/30 (17%)	59/117 (50%)	68/183 (37%)
Night	4/32 (13%)	5/41 (12%)	41/199 (41%)	50/172 (29%)
Total	8/68 (12%)	10/71 (14%)	100/216 (46%)	188/355 (33%)

*Number of fire observations identified by satellite/total fire observations.

TABLE 5. Fraction* of unobstructed fire observations identified by satellite.

	Class 1 (<4 ha)	Class 2 (4–40 ha)	Class 3 (>40 ha)	Total
Day	4/7 (57%)	5/9 (56%)	59/62 (95%)	68/78 (87%)
Night	4/5 (80%)	5/15 (33%)	41/49 (84%)	50/69 (73%)
Total	8/12 (75%)	10/24 (42%)	100/111 (90%)	118/147 (80%)

*Number of fire observations identified by satellite/number of fire observations visible to the satellite.

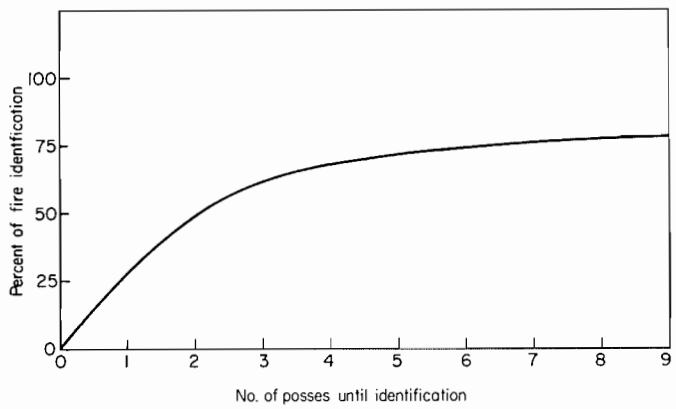

FIG. 8. Percent of fires identified versus the number of satellite passes.

A summation of individual fire identification (not fire observations) versus time for all fires, with the exception of "spot" fires, (0.5 ha or less) is shown in Fig. 8. Approximately 50% of the fires were identified by the second pass. Twenty-five percent of the fires were never detected by satellite. Of these undetected fires, 50% were under 2 ha in size and 75% were available for detection in four passes or less.

The mean fire size as calculated from satellite monitoring is given in Table 6. The bias is the difference between the area observed by the Alberta Forestry Service and the satellite estimate. The estimated fire size was about 70% too large for small fires and about 50% too small for large fires. The statistics on fire size were significantly affected by a few large outliers, where there were significant errors in estimated size.

Sources of error

The forestry data provided by the Alberta Forestry Service is one of many potential sources of error. The size of the fire determined by aircraft reconnaissance is in itself an estimate. Confidence is particularly low when significant quantities of smoke or low cloud exist near the fire site. Daily observations from the Alberta Forestry Service versus 12-h satellite observations created a potential source of error when fires were spreading rapidly. Fires starting or being extinguished between satellite passes constitute another source of error.

TABLE 6. Fire size statistics

	Mean (ha)	Bias (ha)
Day	2875	−1034
Night	1843	−1160
Small fire (≤400 ha)	186	135
Large fire (≥400 ha)	4336	−2059
Total	2467	−1084

Other sources of error are generated by the fire-monitoring technique. The location of the fire within the pixel cannot be identified using this technique. Fires that occur in cloudy areas may be visible to the satellite but be eliminated by the cloud discrimination technique. For example, near the center of Fig. 9 the indicated fire is visible but was not identified by the fire-monitoring technique because the pixels were partially obscured by smoke and cloud. Other fires may have been missed because they were hidden by the forest canopy. Some fires could have gone undetected if the temperature difference between channels 3 and 4 was below the critical threshold. False alarms were caused by heated soil over agricultural land, buildings or pavement in settlement areas, and factory locations. A foreknowledge of the surface cover, settlement, and industrial locations can reduce this type of error. Errors occur in the estimate of fire size by satellite because only the leading edge of large fires is burning whereas large areas of burned over land enclosed by the fire front may have cooled enough to make identification difficult. Finally, the assumption than an entire pixel is homogeneously composed of either fire or unburned forest is not necessarily true. A pixel can contain fire, burned-over forest, unburned forest, smoke, water, and small clouds or any combination of these. Another source of error were limitations of the AVHRR. Saturation of the channel 3 sensor in the AVHRR occurred when the sensed temperature of the entire pixel was greater than 322 K. Saturation does not affect the ability to identify fires but adds uncertainty to the estimation of fire size. Saturation was infrequent during this study and was present in less than 0.1% of the pixels.

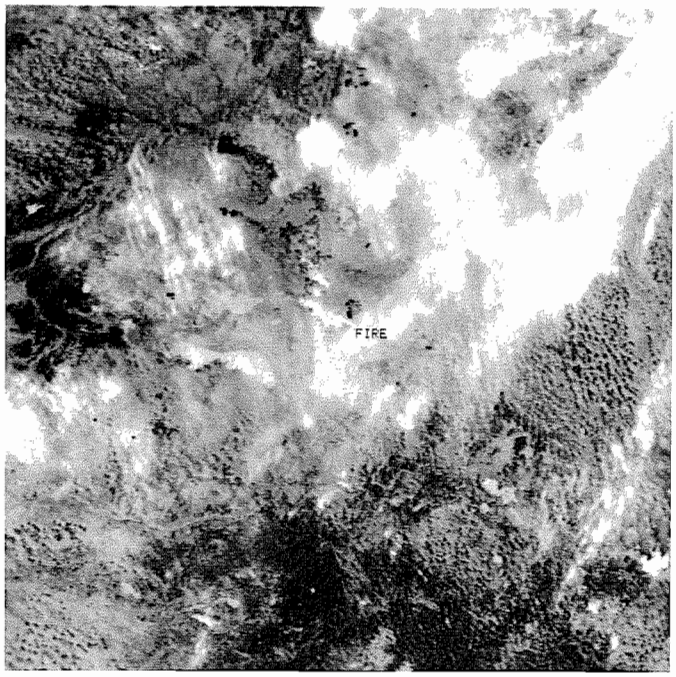

FIG. 9. NOAA-7 pass 5074, AVHRR channel 3, June 17, 1982, 1534 MDT, covering the Slave Lake Forest Region.

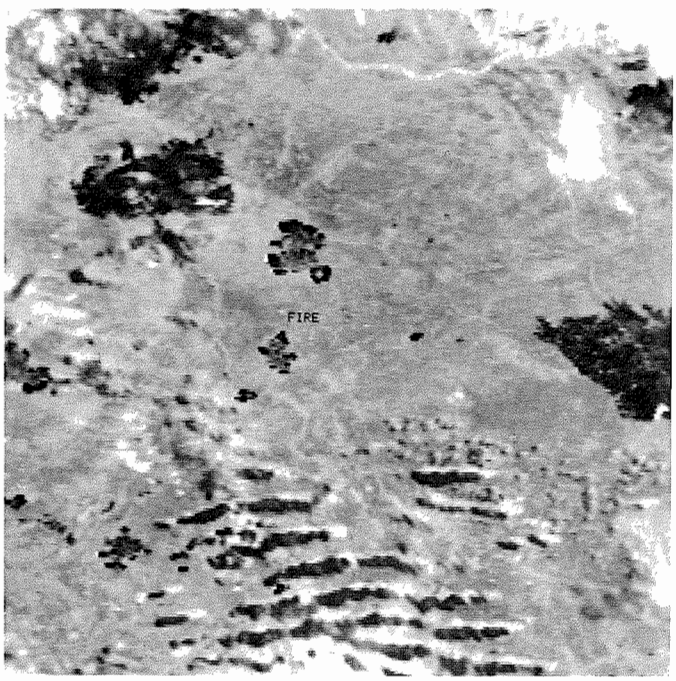

FIG. 10. NOAA-7 pass 5102, AVHRR channel 3, June 19, 1982, 1510 MDT. This is a two-times enlargement of the upper right portion of Fig. 6 showing active fire areas in two major fires near the centre of the image.

Future research

Man–machine interaction combined with masks for agricultural, urban, and previously burned areas would permit the monitoring of cloud and smoke areas for more subtle clues than can be handled automatically.

The fire-monitoring technique should be tested at the ground station closest to the trial region where many components needed by the monitoring technique, such as programs for instrument calibration and temperature and radiance calculations, are already in place. Transmission of fire size and location as well as the actual images could be from the ground station to the appropriate fire control agency in almost real time. A second approach would be to have the image data transmitted directly to the user for processing. To obtain a valid test, the operational trial should monitor forest fires in forested regions with a high fire danger rating (Canadian Forestry Service 1984; Van Wagner and Pickett 1985).

Information from satellite images could help in fire control by identifying where a fire is most active. For example, hot spots where fires are burning most vigorously can be identified near the center of Fig. 10 (a two-times enlargement of a portion of Fig. 6).

Conclusions

Information gained from the fire-monitoring technique described herein could be used to complement existing information available to fire control agencies. During this study, in the absence of cloud and smoke cover, 80% of fire observations reported by the Alberta Forestry Service were identified by satellite. The mean estimated fire size was within 50% of the reported mean fire size for large fires. This additional information could be significant in the protection of life, property, and valuable forest stands.

BELL, G. J., and M. C. WONG. 1981. The near-infrared radiation received by satellites from clouds. Mon. Weather Rev. **109**: 2158–2163.

CANADIAN FORESTRY SERVICE. 1984. Tables for the Canadian Forest Fire Weather Index System. 4th ed. Can. For. Serv., For. Tech. Rep. No. 25

CLARK, J. D. 1983. The GOES user's guide. NOAA, National Environmental Satellite Data and Information Service, Washington DC.

COAKLEY, J. A., JR., and F. P. BRETHERTON. 1982. Cloud cover from high-resolution scanner data: detecting and allowing for partially filled fields of view. J. Geophys. Res. **87**: 4917–4932.

DESCHAMPS, P. Y., and T. PHULPIN, 1980. Atmospheric correction of infrared measurements of sea surface temperature using channels at 3.7, 11 and 12 μm. Boundary-Layer Meteorol. **18**: 131–143.

DOZIER, J. 1981. A method for satellite identification of surface temperature fields of subpixel resolution. Remote Sens. Environ. **11**: 221–229.

GATES, D. M. 1965. Radiant energy, it's receipt and disposal. *In* Agricultural meteorology. *Edited by* P. E. Waggoner. American Meteorological Society, Boston, MA.

FLANNIGAN, M. D. 1985. Forest fire monitoring using the NOAA satellite series. M.S. thesis, Colorado State University, Fort Collins, CO.

HALL, D.K., J. P. ORMSBY, L. JOHNSON, and J. BROWN. 1979. Landsat digital analysis of the initial recovery of the Kokolik River tundra fire area, Alaska. NASA Tech. Memo. No. 80602.

HILLGER, D.W. 1983. Mesoscale moisture fields retrieved from satellite infrared radiances in nocturnal inversion cases. Colo. State Univ., Atmos. Sci. Pap. No. 373.

HORNBECK, R. W. 1975. Numerical methods. Quantum Publishers Inc., New York.

KIDWELL, K. B. 1984. NOAA polar orbiter data (TIROS-N, NOAA-6, NOAA-7, and NOAA-8) user's guide. National Environmental Satellite Data and Information Service, Washington, DC.

KONDRAT'EV, K. YA. 1973. Radiation characteristics of the atmosphere and the earth's surface. Amerind Publishing Co. Ltd., New Delhi, India.

LAURITSON, L., G. J. NELSON, and F. W. PORTO. 1979. Data

extraction and calibration of TIROS-N/NOAA radiometers. NOAA Tech. Mem. NESS-107.

LEE, R. 1978. Forest microclimatology. Columbia University Press, New York.

LLEWELLYN-JONES, D. T., P. J. MINNETT, R. W. SAUNDERS, and A. M. ZAVODY. 1984. Satellite multispectral infrared measurements of sea surface temperature of the N.E. Atlantic Ocean using AVHRR/2. Q. J. R. Meteorol. Soc. **110**: 613–631.

MATSON, M., and J. DOZIER. 1981. Identification of subresolution high temperature sources using a thermal IR sensor. Photogramm. Eng. Remote Sens. **47**: 1311–1318.

MATSON, M., S. R. SCHNEIDER, B. ALDRIDGE, and B. SATCHWELL. 1984. Fire detection using the NOAA-series satellites. NOAA Tech. Mem. NESDIS-7.

RAMSEY, G. S., and D. G. HIGGINS. 1985. Canadian forest fire statistics. Can. For. Serv., Petawawa Natl. For. Inst., Inf. Rep. PI-X-49.

SCHWALB, A. 1978. The TIROS-N/NOAA A-G satellite series. NOAA Tech. Mem. NESS-95.

——— 1982. Modified version of the TIROS N/NOAA A-G satellite series (NOAA E–J)—advanced TIROS N (ATN). NOAA Tech. Mem. NESS-116.

TAPPAN, G., and G. E. MILLER. 1982. Area estimation of environmental phenomena from NOAA-*n* satellite data. NASA, Houston, TX.

VAN WAGNER, C. E., and T. L. PICKETT. 1985. Equations and FORTRAN program for the Canadian Forest Fire Weather Index System. Can. For. Serv., For. Tech. Rep. No. 33.

WONG, C. L., and W. R. BLEVIN, 1967. Infrared reflectances of plant leaves. Aust. J. Biol. Sci. **20**: 501–508.